



Preparation of regenerated cellulose/montmorillonite nanocomposite films via ionic liquids

Shaya Mahmoudian^{a,b}, Mat Uzir Wahit^{a,*}, A.F. Ismail^c, A.A. Yussuf^d

^a Enhanced Polymer Research Group (EnPRO), Department of Polymer Engineering, Faculty of Chemical Engineering, Universiti Teknologi Malaysia (UTM), Johor, Malaysia

^b Department of Textile Engineering, Kashan Branch, Islamic Azad University, Kashan, Iran

^c Advanced Membrane Technology Research Centre (AMTEC), Universiti Teknologi Malaysia (UTM), Johor, Malaysia

^d Petroleum Research and Studies Center, Kuwait Institute for Scientific Research, Kuwait

ARTICLE INFO

Article history:

Received 16 November 2011

Received in revised form 27 January 2012

Accepted 30 January 2012

Available online 7 February 2012

Keywords:

Regenerated cellulose

Montmorillonite

Ionic liquids

Nanocomposite films

ABSTRACT

Regenerated cellulose/montmorillonite (RC/MMT) nanocomposite films were successfully prepared in ionic liquid, 1-butyl-3-methylimidazolium chloride (BMIMCl) using solution casting method. The effect of MMT loading on the thermal, mechanical, gas permeability and water absorption properties of the nanocomposite films was investigated. X-ray diffraction analysis revealed a cellulose II crystalline structure and well dispersed MMT in RC/MMT nanocomposite films. Presence of MMT enhanced the thermal and thermal-oxidative stability and char yield of RC. The tensile strength and Young's modulus of RC films improved by 12% and 40%, respectively with the addition of 6 wt.% MMT. RC/MMT nanocomposite films exhibited improved gas barrier properties and water absorption resistance compared to RC. The results demonstrated that there is a possible interface interaction between cellulose and MMT which yielded better thermal and mechanical properties of the nanocomposite films as compared to pure cellulose.

© 2012 Elsevier Ltd. All rights reserved.

1. Introduction

In recent years biopolymers from renewable resources have attracted much interest as alternative for petroleum based polymers due to increasing environmental concerns and decreasing fossil resources (Sinha Ray & Bousmina, 2005; Vroman & Tighzert, 2009). Cellulose is the most abundant natural polymer in nature and it is currently one of the most promising polymeric resources, being the component of paper, textiles, membranes, artificial fibers, etc. Cellulose which is a linear polymer of β -1,4-linked D-glucopyranose monomers, has many attractive properties such as, biodegradability, renewability, biocompatibility, non toxicity and low cost (Klemm, Heublein, Fink, & Bohn, 2005; Simkovic, 2008). However, the processing of cellulose is difficult in general. Cellulose is neither maltable nor soluble in water or common solvents due to its partially crystalline structure and close chain packing via numerous inter- and intra-molecular hydrogen bonds. The major setback to the more extensive use of cellulose is the lack of suitable solvent for cellulose regeneration process. (Bredereck & Hermanutz, 2005; Klemm, Philipp, Heinze, Heinze, & Wagenknecht, 1998).

For more than one century, the polluting and multistep viscose process was the main technique for cellulose regeneration and it is still applied for the production of regenerated cellulose fibers and films (Louis, 1950; Woodings, 2002). Currently, several cellulose solvent systems have been available for the preparation of regenerated cellulose materials. Among them, N-methylmorpholine-N-oxide (NMMO)/water is commercialized as an environmentally acceptable solvent system (Chanzy, Peguy, Chaunis, & Monzie, 1980; Fink, Weigel, Purz, & Ganster, 2001). However, NMMO/water system have some limitations associated with its use, such as the high temperature required for the dissolution, the degradation of cellulose, the side reactions of solvent itself without an antioxidant, and its high cost (Rosenau, Potthast, Sixta, & Kosma, 2001; Zhang, Wu, Zhang, & He, 2005).

Recently, room temperature ionic liquids (ILs) have been used as 'green' solvents for cellulose regeneration due to their attractive properties such as good chemical and thermal stability, low flammability, low melting point and ease of recycling. Ionic liquids have no measurable vapor pressure and therefore no volatile organic compounds emission to the atmosphere, which makes them as environmentally friendly solvents (Olivier-Bourbigou, Magna, & Morvan, 2009; Rogers & Seddon, 2003; Swatloski, Spear, Holbrey, & Rogers, 2002; Welton, 1999). Swatloski et al. (2002) reported for the first time that ionic liquid 1-butyl-3-methylimidazolium chloride (BMIMCl) has a good dissolving power for cellulose which opened up a new way of developing a class of cellulose solvent systems and promoted several other groups to

* Corresponding author at: Department of Polymer Engineering, Faculty of Chemical Engineering, Universiti Teknologi Malaysia (UTM), 81310 Skudai, Johor, Malaysia. Tel.: +60 7 553 5909; fax: +60 7 553 6165.

E-mail address: mat.uzir@cheme.utm.my (M.U. Wahit).

test a variety of other ILs on their ability to dissolve cellulose. (Feng & Chen, 2008; Liu et al., 2012; Ren, Wu, Zhang, He, & Guo, 2003; Zavrel, Bross, Funke, Büchs, & Spiess, 2009).

Incorporation of nanofillers into polymer matrix has been proved to be a powerful tool to increase the polymer properties. During the past several years, different nanofillers such as carbon nanotube (Kim, Park, Kim, & Park, 2010; Rahatekar et al., 2009; Zhang et al., 2007), nano-carbon black (Vorbach & Taeger, 1998; Zhang, Guo, Shao, & Hu, 2006), graphite oxide (Han, Yan, Chen, Li, & Bangal, 2011), nanohydroxyapatite (Tsioplias & Panayiotou, 2008; Zadeegan, Hosainipour, Rezaie, Ghassai, & Shokrgozar, 2011) and nanoclay (Cerruti et al., 2008; Delhom, White-Ghoorahoo, & Pang, 2010; Lee, Sun, & Deng, 2008; Melle, Mooz, & Meister, 2006) have been used to enhance the thermal and physical properties of regenerated cellulose (RC). Of particular interest are polymer nanocomposites reinforced with organically modified layered silicate such as montmorillonite (MMT). MMT with nano-sized layered structure has a large surface area providing sufficient interfacial regions in polymer nanocomposites which offer tremendous improvement in wide range of physical and engineering properties for polymers with low filler (MMT) loadings. Polymer/MMT nanocomposite materials are believed to have strong potential to widen polymer nanocomposites applications (Sinha Ray & Okamoto, 2003; Zeng, Yu, Lu, & Paul, 2005). Previous study by Cerruti et al. (2008) reported a significant enhancement in thermal stability of regenerated cellulose with the incorporation of MMT using NMMO/water as the solvent. However as mentioned earlier, NMMO/water system have some drawbacks such as cellulose degradation and side reactions of solvent.

At present, and to the best of our knowledge, no study has been reported on cellulose regeneration using ionic liquids for the development of regenerated cellulose/montmorillonite (RC/MMT) nanocomposite films. This novel work presents a facile approach to environmentally friendly preparation of RC/MMT nanocomposites by incorporation of MMT into cellulose matrix using ionic liquid, BMIMCl as solvent. The morphology of RC and RC/MMT nanocomposite films was characterized by X-ray diffraction. Thermal stability, gas permeability, water absorption and mechanical properties of the films were also studied.

2. Experimental

2.1. Materials

Microcrystalline cellulose, a commercial reagent from Sigma with average powder size of 50 μm , Avicel type with the degree of polymerization of 350 was used. Ionic liquid, 1-butyl-3-methylimidazolium chloride (BMIMCl) with purity of $\geq 95\%$ was supplied by Sigma Aldrich. Organo-modified montmorillonite, Nanomer 1.30TC was obtained from Nanocor Inc. (Arlington Heights IL, USA.) Nanomer 1.30TC is organically modified with around 30 wt.% of octadecylamine.

2.2. Preparation of nanocomposite films

Cellulose/MMT nanocomposite films were prepared according to the following procedure; dried (3 h at 70 °C) cellulose was dissolved in ionic liquid BMIMCl with magnetic stirring for 4 h at 85 °C. Meanwhile MMT nanoclays were dispersed in BMIMCl using a sonicator (Model FB15053, Fisher Scientific Co., Germany) for 30 min and then stirring for 4 h at 85 °C. Two solutions were mixed and stirred for 24 h at 85 °C to get a homogenous cellulose/MMT/ionic liquid solution with cellulose concentration of 8 wt.%. After degassing the solution in vacuum oven, it was casted on a glass plate with thickness of about 0.3 mm and immersed immediately into distilled water bath at room temperature for 24 h. The obtained nanocomposite films were washed with running water and dried in a vacuum oven at 30 °C for 3 h. All the dried films were stored in a moisture controlled desiccators until tested. The RC/MMT nanocomposites films prepared by different MMT contents (2, 4, 6 and 8 wt.%) were coded as RC/MMT-2, RC/MMT-4, RC/MMT-6 and RC/MMT-8, respectively. Fig. 1 shows the preparation procedure and optical photographs of RC film and RC/MMT-4 nanocomposites film with an approximate thickness of $\sim 35 \mu\text{m}$.

2.3. Characterization

Contact angle test was performed using sisal drop method on DropMeter A-100 contact angle system (Maist Vision Inspection & Measurement Co. Ltd.) to characterize the nanocomposite films' wetting behavior. The nanocomposite films (70 mm \times 20 mm \times 0.03 mm) were placed on a rectangular glass slide and deionized water droplets were deposited on the films surface at 5 different points using a microsyringe. The contact angles were measured at room temperature and the average of the measured values were taken as its water contact angle.

X-ray diffractometry (XRD) was performed on a Siemens (Berlin, Germany) D5000 X-ray diffractometer with Cu-K α radiation. The X-ray diffraction patterns were recorded with a step size of 0.05° and scanning speed of 0.02°/min from $2\theta = 2$ to 40°. The wave length of X-ray beam is 0.15147 nm.

Thermogravimetric analysis (TGA) tests were carried out on a Perkin Elmer TGA 7 (Perkin Elmer Instruments, USA) with heating rate of 10 °C/min at temperature range from 25 to 650 °C in both in nitrogen and oxygen environment. Approximately 10 mg of samples was used with gas flow rate of 50 mL/min.

Tensile testing was performed on a LRX Tensile Testing Machine (Lloyd, USA) according to ASTM D882-10 with crosshead speed of 10 mm/min. A gauge length of 25 mm was used. All specimens were cut into strips of 60 mm \times 13 mm \times 0.03 mm. Five specimens of each formulation were tested and the average values were reported. All measurements were performed at 23 °C with relative humidity of 60%.

Oxygen and carbon dioxide permeability rates were measured using a constant-pressure system and a soap bubble flow meter. The permeation tests were carried out at 25 °C with feed gas pressure of

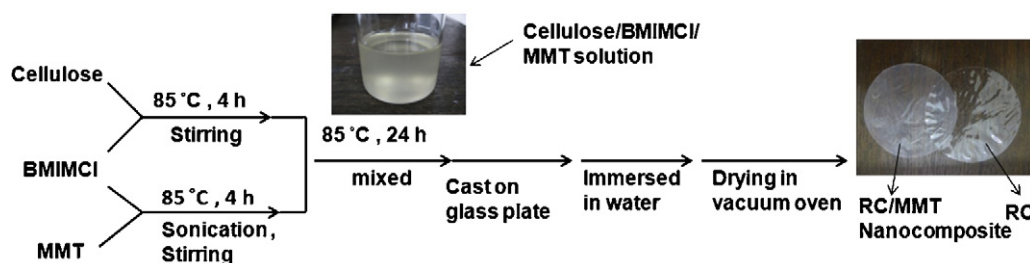


Fig. 1. Preparation procedure of RC/MMT nanocomposite films using ionic liquid, BMIMCl.

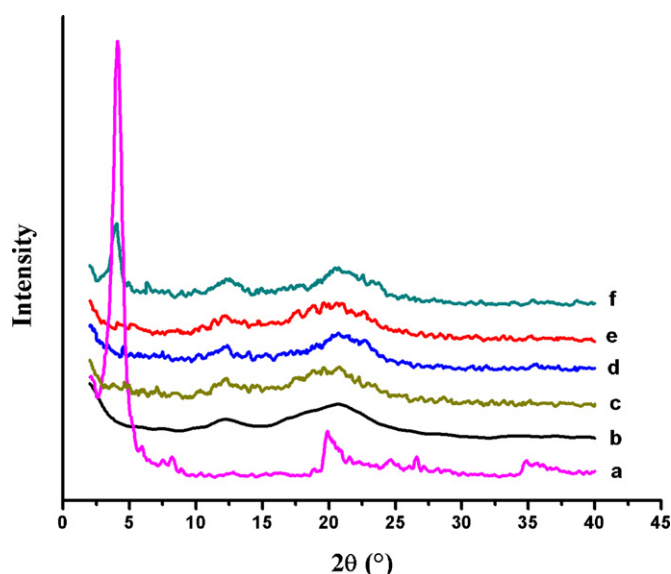


Fig. 2. XRD patterns of MMT 1.30TC (a), pure RC film (b), RC/MMT-2 (c), RC/MMT-4 (d), RC/MMT-6 (e) and RC/MMT-8 (f).

5 bar gauge. The measurement was repeated three times for each sample. The pure gas permeability was calculated using Eq. (1):

$$P = \frac{l}{A\Delta p} \frac{dV}{dt} \quad (1)$$

where P is the permeability, Δp is the pressure difference across films (Pa), A is the effective surface area ($12.5 \times 10^{-4} \text{ m}^2$), l is the thickness of nanocomposites (m), t is the permeation time (s), V is the volume of the gas permeated through the membrane ($\text{m}^3_{(\text{STP})}$).

Water absorption test was conducted according to ASTM D570-98. The samples ($76.2 \text{ mm} \times 25.4 \text{ mm} \times 0.03 \text{ mm}$) were dried to a constant weight under vacuum prior to immersion in distilled water at 25°C for 2 and 24 h. Weight gain of the samples were recorded by removal of the specimens from immersion and weighed. The average value for five samples from every formulation was reported. The % weight gain was determined by Eq. (2).

$$\% \text{ weight gain} = \frac{(W_w - W_d)}{W_d} \times 100 \quad (2)$$

where, W_d and W_w are the weights of dry (before immersion) and wet (after immersion) materials, respectively.

3. Results and discussion

3.1. X-ray diffraction analysis

The XRD patterns of MMT, RC and RC/MMT nanocomposite films with different MMT loadings are shown in Fig. 2. The diffraction pattern of organo-modified MMT exhibited a diffraction peak at $2\theta = 4.1^\circ$, corresponding to interlayer spacing of (001) plane with distance of 21.2 \AA for alkylammonium modified silicate. In the absence of organomodifiers, the interlayer spacing of MMT is in the range of $9.5\text{--}15 \text{ \AA}$ depending on the interlayer ions (Ca^{2+} , Na^+ , etc.). Substitution of these ions with bulky alkyl chains (MMT modification) leads to an increase in the interlayer spacing, which would favor polymer chains to enter into the interlayer-gallerie of MMT (Cerruti et al., 2008; Xu, Bao, & He, 2002). In RC, the peak at $2\theta = 12.2^\circ$ assigned to (1 $\bar{1}$ 0) plane and the broad reflection peak at around $2\theta = 20.5^\circ$ are assigned to the (1 1 0)/(0 2 0) lattice planes of known cellulose II crystalline structure (Chen et al., 2006; Ruan et al., 2006).

The diffraction peak of RC/MMT-2, RC/MMT-4 and RC/MMT-6 nanocomposite films are similar to that of pure RC and the diffraction peak of MMT 1.30TC at $2\theta = 4.1^\circ$ is not observed, which suggests that parallel form of MMT stacking was totally disrupted which gives an indication of MMT exfoliation into cellulose matrix. Lee et al. (2008) also showed that the absence of MMT peak in cellulose/MMT nanocomposite material demonstrates a true nanocomposite with exfoliated MMT in cellulose matrix. The effect of different nanoparticles on the RC matrix structure after the incorporation was studied by Melle et al. (2006). Their XRD patterns showed that regenerated cellulose/MMT films with 4 wt.% MMT attained good exfoliation of MMT in the nanocomposite film.

The appearance of cellulose crystalline peak at around $2\theta = 20.5^\circ$ in RC/MMT nanocomposite films shows that no obvious crystal orientation change in cellulose occurred by the incorporation of MMT. In RC/MMT-8 nanocomposite film, the weak peak at $2\theta = 4.05^\circ$ represents the interlayer spacing of stacked MMT layers which is an evidence of MMT agglomeration in the RC matrix. Previous study also reported that, with MMT concentration of higher than 6 wt.%, it tends to agglomerate or flocculate in cellulose matrix (Lee et al., 2008).

3.2. Thermal stability analysis

Thermal-degradation of RC and RC/MMT nanocomposites was studied by thermogravimetric analysis under nitrogen and Oxygen environments to determine the effect of MMT on thermal stability of RC. The traces recorded at $10^\circ\text{C}/\text{min}$ for RC and RC/MMT nanocomposites are reported in Fig. 3(a) and (b). The thermal stability is characterized by the temperatures at 10%, 20% and 80% weight losses occurred, referred to as T_{10} , T_{20} and T_{80} (data are shown in Table 1). It can be observed that the incorporation of MMT improved the decomposition temperature in RC/MMT nanocomposites. The thermal stability of nanocomposites increased with increasing MMT, up to a loading of 6 wt.%. From Fig. 3(a), it can be seen that, the T_{20} of RC films improved around 10°C from 299.9°C to 309.4°C with 6 wt.% MMT content. It is believed that MMT platelets (impermeable) increased the thermal stability of cellulose, by providing hindrance to the diffusion of heat mass transfer (out-migration of degraded volatiles) to the surface, thus retarding the decomposition rate (Sinha Ray & Okamoto, 2003). Previous studies on cellulose/MMT nanocomposites also reported similar results (Cerruti et al., 2008; Delhom et al., 2010).

The thermal stability of RC/MMT nanocomposites dropped slightly at RC/MMT-8 nanocomposite. According to Sinha Ray and Okamoto (2003), the increase in degradation temperature of polymer/MMT nanocomposites is also attributed to the good dispersion and exfoliation of MMT in polymer matrix. Therefore this reduction in thermal stability is perhaps due to the poor dispersion and agglomeration of MMT in RC/MMT-8 as also confirmed by XRD analysis. The agglomeration reduces MMT's surface area available for char formation; therefore thermal stability of the nanocomposite reduces. Delhom et al. (2010) also reported a decrease in degradation temperature of cotton/MMT nanocomposites at higher contents of MMT.

TGA curve of RC and RC/MMT nanocomposites underwent double decomposition steps in oxygen rich environment (Fig. 3(b)). The first stage weight loss is due to the oxidation of cellulose, which was also reported by Cerruti et al. (2008) while the second stage is attributed to the decomposition of chars. At the second weight loss step which occurs at the range of $300\text{--}500^\circ\text{C}$, cellulose nanocomposites showed slower decomposition rate due to the increased stability. The presence of MMT also enhanced RC thermo-oxidative stability. It can be seen that, the T_{10} value of RC films (245°C) improved by about 32°C to 277.8°C with 6 wt.% of MMT loading.

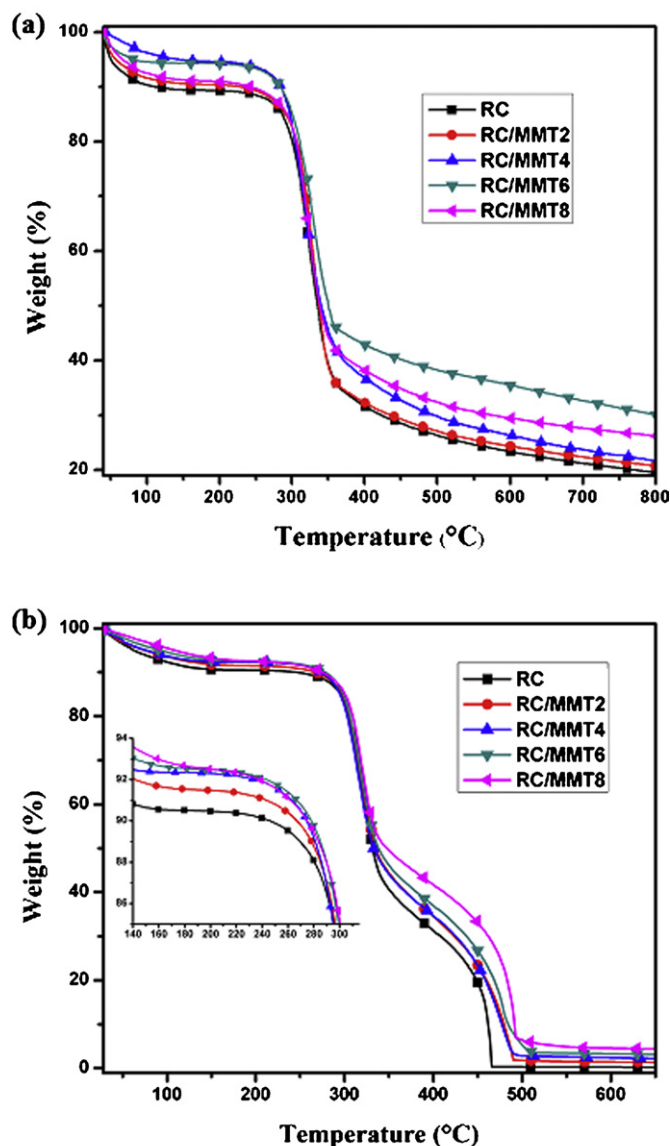


Fig. 3. TGA curves of RC/MMT nanocomposites with various MMT loadings under nitrogen environment (a) and oxygen environment (b).

It is reasonable that the presence of MMT also hinder the oxygen diffusion and retards the thermal transfer into the polymer matrix.

The char yields at 650 °C for RC and RC/MMT nanocomposite are also shown in Table 1. The char yield is higher for RC nanocomposite films as compared to RC films in both nitrogen and oxygen environments and it increased by increasing the MMT loading. The char yield of RC film at 650 °C was about 22.1 wt.% and 0.13 wt.% in nitrogen and oxygen rich environment, respectively, whereas it was 28.4 wt.% and 4.8 wt.% for RC/MMT-8. It can be seen that

the char yield percentage by weight is lower than actual MMT weight added during preparation. This weight loss of 30–40 wt.% is perhaps due to the decomposition of octadecylamine which was added into MMT 1.30TC galleries during its modification (Wilkinson et al., 2006). The remaining char is attributed to the high thermal stability of MMT (Sinha Ray & Okamoto, 2003).

3.3. Mechanical properties

Fig. 4(a) shows the effect of MMT content on tensile strength and elongation at break of RC and RC/MMT nanocomposites. It can be observed that the addition of MMT increased tensile strength of the films. The RC/MMT-6 exhibited about 12% increase in the tensile strength. As the MMT loading further increased, the tensile strength decreased, which is attributed to the aggregation of MMT particles. Previous studies also reported that higher contents of MMT (>5 wt.%) in polymer can result in its agglomeration resulting in deprived mechanical performance compared to lower contents (Lee et al., 2008; Wilkinson et al., 2007). The elongation at break values of RC/MMT nanocomposites however, decreased with the presence of MMT. The elongation at break values of the films decreased from 7.5% to 4.5% as the MMT content increased from 0 to 8 wt.%. This could be attributed to the presence of MMT which restrains the slippage movement of RC chains during deformation and therefore resulting in decreased elongation at break values.

Fig. 4(b) illustrates the dependence of Young's modulus on the MMT content. The Young's modulus of RC films increased linearly with increasing MMT loadings. The RC/MMT-6 nanocomposite film exhibited about 40% increase in modulus compare to the pure RC films. The improvement in modulus of RC is due to the high rigidity exerted by the MMT as it does not deform or relax and therefore the cellulose's chain movement was suppressed by MMT particles. This improvement in modulus may also be ascribed to the dispersion and alignment of MMT platelets within cellulose. As when MMT particles disperse in intercalated or exfoliated form, it will provide higher interfacial region which will make stress transfer to MMT layers more effective. For RC/MMT-8, the rise in modulus is less significant. Reductions in modulus enhancement at higher level of MMT loading was ascribed to reduced level of dispersion. The modulus improvement of polymers provided by incorporation of MMT had also been reported by many researchers (Yang, Wang, & Wang, 2007). Lee et al. (2008) found that the presence of MMT at 2 wt.% in RC/MMT nanocomposites prepared via NMMO, enhanced Young's modulus by 10–20% for different types of MMT.

3.4. Gas permeability

Oxygen (O₂) and carbon dioxide (CO₂) permeability values of RC film and RC/MMT nanocomposite films are presented in Table 2. Permeability values decreased gradually with increasing MMT concentration. O₂ and CO₂ Permeability decreased by about 33% and 31%, respectively by addition of 6 wt.% MMT. The reduction in permeability is attributed to the high aspect ratio of MMT

Table 1
TGA results of RC and RC/MMT nanocomposites films.

Samples	Oxygen environment			Nitrogen environment		
	T ₁₀ (°C)	T ₈₀ (°C)	Residue (%) at 650 °C	T ₁₀ (°C)	T ₂₀ (°C)	Residue (%) at 650 °C
RC	245.0	446.7	0.13	111.9	299.9	22.1
RC/MMT-2	266.0	458.0	1.4	229.3	305.3	23.2
RC/MMT-4	273.0	457.9	2.2	283.7	304.0	24.9
RC/MMT-6	277.8	468.8	3.8	284.0	309.4	34.0
RC/MMT-8	274.8	483.8	4.8	242.0	306.0	28.4

Table 2
Gas permeability of RC and RC/MMT nanocomposite films.

Samples	Oxygen permeability ($\times 10^{-18}$ m ³ m/m ² s Pa)	Carbon dioxide permeability ($\times 10^{-18}$ m ³ m/m ² s Pa)	Permeability ratio (PCO ₂ /PO ₂)
RC	1.12 \pm 0.04	1.85 \pm 0.04	1.65
RCMMT-2	1.03 \pm 0.10	1.45 \pm 0.07	1.40
RCMMT-4	0.84 \pm 0.13	1.36 \pm 0.11	1.61
RCMMT-6	0.76 \pm 0.11	1.26 \pm 0.06	1.65
RCMMT-8	0.82 \pm 0.08	1.34 \pm 0.12	1.63

particles combined with intercalation of MMT in cellulose matrix, which resulted in an increase in tortuosity, and increasing MMT volume fraction improves this property (Arora & Padua, 2010; Choudalakis & Gotsis, 2009; Silvestre, Duraccio, & Cimmino, 2011). Previous studies on different polymers/MMT nanocomposites such as poly(lactic acid) (Emilie, Eliane, & René, 2011; Koh et al., 2008), polyurethane (Osman, Mittal, Morbidelli, & Suter, 2003), polyimide (Min, Kim, & Chang, 2011) and polyethylenimine (Priolo, Holder, Gamboa, & Grunlan, 2011) also showed that MMT can be a good candidate to reduce the polymer gas permeability.

It was found that permeability of CO₂ through RC and RC/MMT nanocomposites is higher compared to O₂. The CO₂/O₂ permeability ratio were in the range of 1.40–1.64. This ratio has an implication in designing films/coating suitable for fruits and vegetables. Higher

Table 3

Water contact angle and water absorption rate values of RC and RC/MMT nanocomposites.

Samples	Contact angle		Water absorption (%)	
	1 s/°	10 s/°	2 h	24 h
RC	38.3 \pm 2.2	32.7 \pm 2.4	83.6 \pm 1.5	90.2 \pm 1.7
RC/MMT-2	44.3 \pm 2.8	42 \pm 2.2	57.7 \pm 1.1	65.8 \pm 1.5
RC/MMT-4	55.8 \pm 1.9	52.6 \pm 2.1	56.3 \pm 1.3	62.7 \pm 1.5
RC/MMT-6	78.1 \pm 2.4	72.8 \pm 2.3	55.9 \pm 1.2	58.7 \pm 1.0
RC/MMT-8	79.6 \pm 2.7	73.8 \pm 2.4	56.1 \pm 1.8	61.3 \pm 1.2

ratio will allow less accumulation of CO₂ and vice versa. Higher permeability of CO₂ is due to its smaller kinetic diameter combined with its greater solubility towards cellulose (Wu, Wang, Wang, Bian, & Li, 2009). Previous studies also reported CO₂/O₂ permeability ratio of >1 for regenerated cellulose/soy protein (Wu et al., 2009) and regenerated cellulose/starch/lignin films (Wu, Wang, Li, Li, & Wang, 2008). Wu and Yuan (2002) who also studied gas permeability of regenerated cellulose membrane, reported a higher permeation rate for CO₂ compared to O₂, N₂, CH₄ and H₂.

3.5. Water contact angle

The level of interaction of the RC and RC/MMT films with water was investigated via the contact angle test. The contact angle of water on the surface of RC and RC/MMT nanocomposites are summarized in Table 3. The contact angle values are increased with increasing MMT content up to 8 wt.%. The contact angle of RC film with water was found to be 38.3° and 32.7° in 1 s and 10 s respectively, whereas it was 79.6° and 73.8° for RC/MMT-8. The enhanced contact angle in RC/MMT nanocomposites indicates the increase in hydrophobicity which is due to the lower hydrophilicity of MMT particles than that of cellulose.

3.6. Water absorption

The water absorption (%) of RC and RC/MMT nanocomposites for 2 h and 24 h are also shown in Table 3. The presence of MMT in cellulose leads to improvement in water resistance for RC/MMT nanocomposite films. The 24 h water absorption of the nanocomposite films decreased from 90.2% to 61.3% as the MMT content increased from 0 to 8 wt.%. It can be deduced that the addition of MMT diminishes the water absorption of the RC films due to the presence of impermeable MMT particles in the nanocomposites which can lower the rate of water transport in the polymer matrix. This may also be attributed to the low maximum water uptake of MMT compared to RC. Similar observation was also reported by other researchers for various polymer/MMT nanocomposites (Cyras, Manfredi, Ton-That, & Vázquez, 2008; Kojima et al., 1993; Liu, Hoa, & Pugh, 2005).

4. Conclusions

Nanocomposite films of cellulose and MMT were successfully prepared using ionic liquid, BMIMCl, as solvent. This is a facile

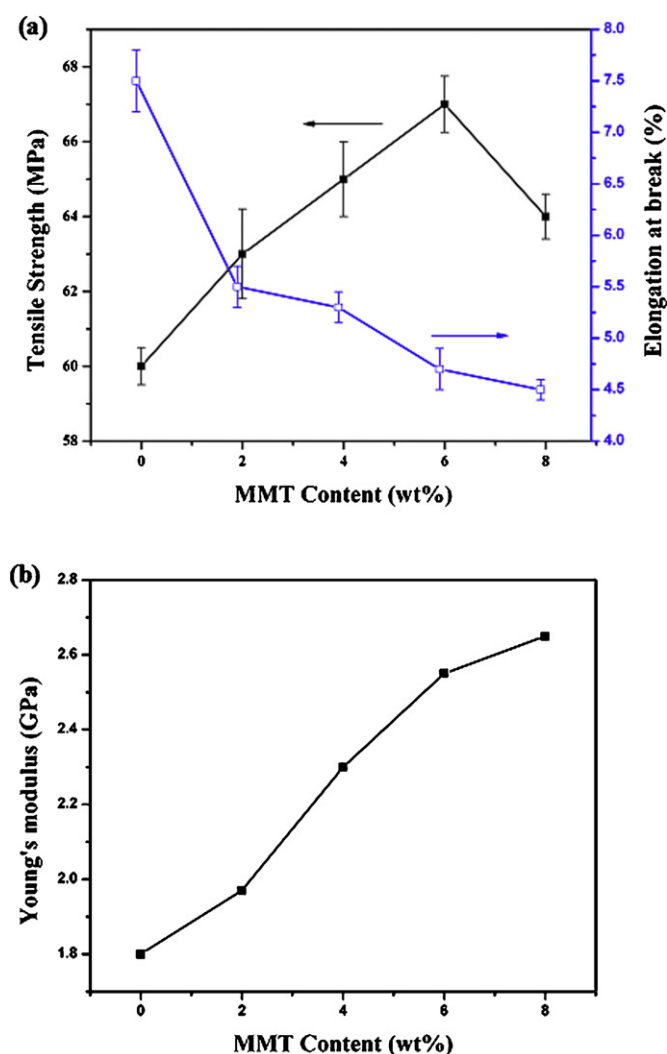


Fig. 4. Effect of MMT contents on tensile strength and elongation at break (a), and Young's modulus (b) of RC/MMT nanocomposite films.

and environmentally friendly method of regeneration cellulose and cellulose nanocomposites. The results revealed improved thermal stability, mechanical and gas barrier properties by incorporation of MMT in to RC matrix. In air environment, the T_{10} value of RC films (245 °C) is improved by about 32 °C to 277.8 °C and the char yield is increased from 0.2 to 4.2 wt.% with 6 wt.% MMT loading. A 12 wt.% increases in tensile strength and a 40% improvement of Young's modulus were also achieved by incorporation of 6 wt.% MMT. Thermal stability and tensile strength of RC/MMT nanocomposites decreased at 8 wt.% of MMT content due to the aggregation of MMT platelets at higher content. Lower water absorption and higher water contact angle revealed an improved hydrophobicity of RC/MMT nanocomposites compared to RC. The development of RC/MMT nanocomposites is expected to play an important role in membrane technology and packaging. The current method used to produce these RC/MMT nanocomposites may also be applicable for the production of other types of nanocomposites, particularly from cellulose.

Acknowledgment

The authors would like to acknowledge the Fundamental Research Grant Scheme (FRGS) Vote No: 78690 by Universiti Teknologi Malaysia from the Ministry of Science, Technology and Innovation (MOSTI).

References

- Arora, A., & Padua, G. W. (2010). Review: Nanocomposites in food packaging. *Journal of Food Science*, 75, 43–49.
- Bredereck, K., & Hermanutz, F. (2005). Man-made cellulose. *Review of Progress in Coloration and Related Topics*, 35, 59–75.
- Cerruti, P., Ambrogio, V., Postiglione, A., Rychlý, J., Matisová, Rychlá, L., & Carfagna, C. (2008). Morphological and thermal properties of cellulose/montmorillonite nanocomposites. *Biomacromolecules*, 9, 3004–3013.
- Chanzy, H., Peguy, A., Chaunis, S., & Monzie, P. (1980). Oriented cellulose films and fibers from a mesophase system. *Journal of Polymer Science: Polymer Physics Edition*, 18, 1137–1144.
- Chen, X., Burger, C., Fang, D., Ruan, D., Zhang, L., Hsiao, B. S., et al. (2006). X-ray studies of regenerated cellulose fibers wet spun from cotton linter pulp in NaOH/thiourea aqueous solutions. *Polymer*, 47, 2839–2848.
- Choudalakis, G., & Gotsis, A. D. (2009). Permeability of polymer/clay nanocomposites: A review. *European Polymer Journal*, 45, 967–984.
- Cyras, V. P., Manfredi, L. B., Ton-That, M.-T., & Vázquez, A. (2008). Physical and mechanical properties of thermoplastic starch/montmorillonite nanocomposite films. *Carbohydrate Polymers*, 73, 55–63.
- Delhom, C. D., White-Ghoorahoo, L. A., & Pang, S. S. (2010). Development and characterization of cellulose/clay nanocomposites. *Composites Part B: Engineering*, 41, 475–481.
- Emilie, P., Eliane, E., & René, F. (2011). Effect of an organo-modified montmorillonite on PLA crystallization and gas barrier properties. *Applied Clay Science*, 53, 58–65.
- Feng, L., & Chen, Z.-I. (2008). Research progress on dissolution and functional modification of cellulose in ionic liquids. *Journal of Molecular Liquids*, 142, 1–5.
- Fink, H. P., Weigel, P., Purz, H. J., & Ganster, J. (2001). Structure formation of regenerated cellulose materials from NMMO-solutions. *Progress in Polymer Science*, 26, 1473–1524.
- Han, D., Yan, L., Chen, W., Li, W., & Bangal, P. R. (2011). Cellulose/graphite oxide composite films with improved mechanical properties over a wide range of temperature. *Carbohydrate Polymers*, 83, 966–972.
- Kim, D. H., Park, S. Y., Kim, J., & Park, M. (2010). Preparation and properties of the single-walled carbon nanotube/cellulose nanocomposites using N-methylmorpholine-N-oxide monohydrate. *Journal of Applied Polymer Science*, 117, 3588–3594.
- Klemm, D., Heublein, B., Fink, H.-P., & Bohn, A. (2005). Cellulose: Fascinating biopolymer and sustainable raw material. *Angewandte Chemie International Edition*, 44, 3358–3393.
- Klemm, D., Philipp, B., Heinze, T., Heinze, U., & Wagenknecht, W. (1998). *Comprehensive cellulose chemistry*. Germany: Wiley-VCH.
- Koh, H. C., Park, J. S., Jeong, M. A., Hwang, H. Y., Hong, Y. T., Ha, S. Y., et al. (2008). Preparation and gas permeation properties of biodegradable polymer/layered silicate nanocomposite membranes. *Desalination*, 233, 201–209.
- Kojima, Y., Usuki, A., Kawasumi, M., Okada, A., Kurauchi, T., & Kamigaito, O. (1993). Sorption of water in nylon 6-clay hybrid. *Journal of Applied Polymer Science*, 49, 1259–1264.
- Lee, J., Sun, Q., & Deng, Y. (2008). Nanocomposites from regenerated cellulose and nanoclay. *Journal of Biobased Materials and Bioenergy*, 2, 162–168.
- Liu, W., Hoa, S. V., & Pugh, M. (2005). Fracture toughness and water uptake of high-performance epoxy/nanoclay nanocomposites. *Composites Science and Technology*, 65, 2364–2373.
- Liu, D. T., Xia, K.-f., Cai, W.-h., Yang, R.-d., Wang, L.-q., & Wang, B. (2012). Investigations about dissolution of cellulose in the 1-allyl-3-alkylimidazolium chloride ionic liquids. *Carbohydrate Polymers*, 87, 1058–1064.
- Louis, C.N. (1950). United States Patent No. 2535044. U.S. Patent.
- Melle, J., Mooz, M., & Meister, F. (2006). Nanoparticle modified cellulose fibres. *Macromolecular Symposia*, 244, 166–174.
- Min, U., Kim, J.-C., & Chang, J.-H. (2011). Transparent polyimide nanocomposite films: Thermo-optical properties, morphology, and gas permeability. *Polymer Engineering & Science*, 51, 2143–2150.
- Olivier-Bourbigou, H., Magna, L., & Morvan, D. (2009). Ionic liquids and catalysis: Recent progress from knowledge to applications. *Applied Catalysis A: General*, 373, 1–56.
- Osman, M. A., Mittal, V., Morbidelli, M., & Suter, U. W. (2003). Polyurethane adhesive nanocomposites as gas permeation barrier. *Macromolecules*, 36, 9851–9858.
- Priolo, M. A., Holder, K. M., Gamboa, D., & Grunlan, J. C. (2011). Influence of clay concentration on the gas barrier of clay-polymer nanobrick wall thin film assemblies. *Langmuir*, 27, 12106–12114.
- Rahatekar, S. S., Rasheed, A., Jain, R., Zammarano, M., Kozioł, K. K., Windle, A. H., et al. (2009). Solution spinning of cellulose carbon nanotube composites using room temperature ionic liquids. *Polymer*, 50, 4577–4583.
- Ren, Q., Wu, J., Zhang, J., He, J., & Guo, M. (2003). Synthesis of 1-allyl-3-methylimidazolium-based room-temperature ionic liquid and preliminary study of its dissolving cellulose. *Acta Polymerica Sinica*, 448–451.
- Rogers, R. D., & Seddon, K. R. (2003). Chemistry: Ionic liquids – solvents of the future? *Science*, 302, 792–793.
- Rosenau, T., Potthast, A., Sixta, H., & Kosma, P. (2001). The chemistry of side reactions and byproduct formation in the system NMMO/cellulose (Lyocell process). *Progress in Polymer Science*, 26, 1763–1837.
- Ruan, D., Zhang, L., Lue, A., Zhou, J., Chen, H., Chen, X., et al. (2006). A rapid process for producing cellulose multi-filament fibers from a NaOH/thiourea solvent system. *Macromolecular Rapid Communications*, 27, 1495–1500.
- Silvestre, C., Duraccio, D., & Cimmino, S. (2011). Food packaging based on polymer nanomaterials. *Progress in Polymer Science*, 36, 1766–1782.
- Simkovic, I. (2008). What could be greener than composites made from polysaccharides? *Carbohydrate Polymers*, 74, 759–762.
- Sinha Ray, S., & Bousmina, M. (2005). Biodegradable polymers and their layered silicate nanocomposites: In greening the 21st century materials world. *Progress in Materials Science*, 50, 962–1079.
- Sinha Ray, S., & Okamoto, M. (2003). Polymer/layered silicate nanocomposites: A review from preparation to processing. *Progress in Polymer Science*, 28, 1539–1641.
- Swatloski, R. P., Spear, S. K., Holbrey, J. D., & Rogers, R. D. (2002). Dissolution of cellulose with ionic liquids. *Journal of the American Chemical Society*, 124, 4974–4975.
- Tsiptsias, C., & Panayiotou, C. (2008). Preparation of cellulose-nanohydroxyapatite composite scaffolds from ionic liquid solutions. *Carbohydrate Polymers*, 74, 99–105.
- Vorbach, D., & Taeger, E. (1998). Properties of carbon filled cellulose filament. *Chemical Fibers International*, 48, 120–122.
- Vroman, I., & Tighzert, L. (2009). Biodegradable polymers. *Materials*, 2, 307–344.
- Welton, T. (1999). Room-temperature ionic liquids. Solvents for synthesis and catalysis. *Chemical Reviews*, 99, 2071–2084.
- Wilkinson, A. N., Man, Z., Stanford, J. L., Matikainen, P., Clemens, M. L., Lees, G. C., et al. (2006). Structure and dynamic mechanical properties of melt intercalated polyamide 6–montmorillonite nanocomposites. *Macromolecular Materials and Engineering*, 291, 917–928.
- Wilkinson, A. N., Man, Z., Stanford, J. L., Matikainen, P., Clemens, M. L., Lees, G. C., et al. (2007). Tensile properties of melt intercalated polyamide 6 – montmorillonite nanocomposites. *Composites Science and Technology*, 67, 3360–3368.
- Woodings, C. (2002). *Cellulose fibers, regenerated encyclopedia of polymer science and technology*. John Wiley & Sons, Inc.
- Wu, H., Wang, X. L., Li, F., Li, H. Z., & Wang, Y. Z. (2008). Green composite films prepared from cellulose, starch and lignin in room-temperature ionic liquid. *Bioresource Technology*, 100, 2569–2574.
- Wu, H., Wang, X. L., Wang, Y. Z., Bian, X. C., & Li, F. (2009). Cellulose/soy protein isolate blend films prepared via room-temperature ionic liquid. *Industrial & Engineering Chemistry Research*, 48, 7132–7136.
- Wu, J., & Yuan, Q. (2002). Gas permeability of a novel cellulose membrane. *Journal of Membrane Science*, 204, 185–194.
- Xu, W.-B., Bao, S.-P., & He, P.-S. (2002). Intercalation and exfoliation behavior of epoxy resin/curing agent/montmorillonite nanocomposite. *Journal of Applied Polymer Science*, 84, 842–849.
- Yang, K.-K., Wang, X.-L., & Wang, Y.-Z. (2007). Progress in nanocomposite of biodegradable polymer. *Journal of Industrial and Engineering Chemistry*, 13, 485–500.
- Zadegan, S., Hosainilipour, M., Rezaie, H. R., Ghassai, H., & Shokrgozar, M. A. (2011). Synthesis and biocompatibility evaluation of cellulose/hydroxyapatite nanocomposite scaffold in 1-n-allyl-3-methylimidazolium chloride. *Materials Science and Engineering: C*, 31, 954–961.
- Zavrel, M., Bross, D., Funke, M., Büchs, J., & Spiess, A. C. (2009). High-throughput screening for ionic liquids dissolving (ligno-)cellulose. *Bioresource Technology*, 100, 2580–2587.

- Zeng, Q. H., Yu, A. B., Lu, G. Q. M., & Paul, D. R. (2005). Clay-based polymer nanocomposites: Research and commercial development. *Journal of Nanoscience and Nanotechnology*, 5, 1574–1592.
- Zhang, H., Guo, L., Shao, H., & Hu, X. (2006). Nano-carbon black filled lyocell fiber as a precursor for carbon fiber. *Journal of Applied Polymer Science*, 99, 65–74.
- Zhang, H., Wang, Z. G., Zhang, Z. N., Wu, J., Zhang, J., & He, J. S. (2007). Regenerated-cellulose/multiwalled- carbon-nanotube composite fibers with enhanced mechanical properties prepared with the ionic liquid 1-allyl-3-methylimidazolium chloride. *Advanced Materials*, 19, 698–704.
- Zhang, H., Wu, J., Zhang, J., & He, J. (2005). 1-Allyl-3-methylimidazolium chloride room temperature ionic liquid: A new and powerful nonderivatizing solvent for cellulose. *Macromolecules*, 38, 8272–8277.